Journal of Medicinal Chemistry

Article

pubs.acs.org/jmc

Detection of *in Vitro* Metabolite Formation of Leflunomide: A Fluorescence Dynamics and Electronic Structure Study

Poornima Sharma,[†] Debraj Gangopadhyay,[†] Phool Chand Mishra,[†] Hirdyesh Mishra,[*,‡] and Ranjan K. Singh[*,†]

[†]Department of Physics, Banaras Hindu University, Varanasi 221005, India

[‡]Physics Department, MMV, Banaras Hindu University, Varanasi 221005, India

Supporting Information

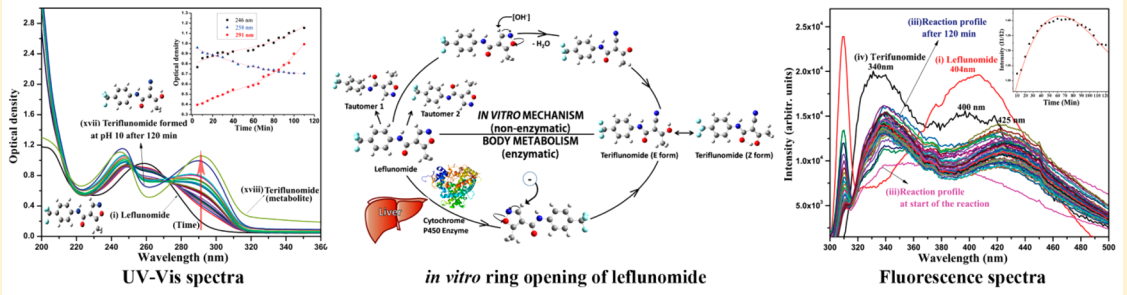

UV-Vis spectra | *in vitro* ring opening of leflunomide | Fluorescence spectra

ABSTRACT: The metabolic transformation of antirheumatic fluorescent drug leflunomide into its active metabolite teriflunomide through isoxazole ring opening has been monitored *in vitro* using steady state and time domain fluorescence spectroscopy and density functional theory. During metabolic reaction, absorption of leflunomide split into two bands resembling absorption spectra of teriflunomide. The fluorescence spectra reveal slow conversion of leflunomide to *E* and *Z* forms of teriflunomide in aqueous medium, which becomes faster at basic pH. The *E* form, which is more potent as a drug, becomes more stable with an increase in the basicity of the medium. Both molecules are associated with charge transfer due to twisting in the lowest singlet excited state. Excited state charge transfer followed by proton transfer was also observed in the *Z* form during the ring opening of leflunomide. Quantum yield and radiative decay rates have been observed to decrease for the metabolite because of an increase in nonradiative decay channels.

INTRODUCTION

Leflunomide {*N*-[(4-trifluoromethyl)phenyl]-5-methylisoxazole 4-carboxamide} is an isoxazole derivative with anti-inflammatory and anticancer activities, and it is commonly used as an antirheumatic drug.[1−9] After intake, it is rapidly transformed into its active metabolite, α-cyanoenol A771726 {2-cyano-3-oxo-*N*-[(4-trifluoromethyl)phenyl]butyramide}, also known as teriflunomide in the gut wall and liver through isoxazole ring opening of leflunomide,[10−12] as shown in the bottom half of Figure 1. Teriflunomide was itself also approved by the U.S. Food and Drug Administration (FDA) in 2012 as an orally administered drug for the treatment for multiple sclerosis.[13,14] The crystal structure and nuclear magnetic resonance (NMR) studies show that teriflunomide interacts with amino acids tyrosine (Tyr356) and arginine (Arg136) in the human enzyme domain dihydroorotate dehydrogenase (DHODH). It is reported that the *E* isomer of teriflunomide interacts more strongly with DHODH than the *Z* isomer does.[15−17] *In silico* studies based on density functional theory (DFT) were recently performed to study the adsorption of leflunomide on carbon nanotubes.[18] DFT-optimized structures of leflunomide, teriflunomide, and the analogues of teriflunomide were reported by Panek et al.[19] Temperature-dependent Raman and X-ray diffraction (XRD) studies have revealed that leflunomide exists in two polymorphic forms α and β, the former being predominantly present at room temperature and the latter occurring at temperatures higher than 373 K. The α and β forms have different hydrogen bonding patterns between monomers.[20,21]

The action of leflunomide as a drug starts after formation of its metabolite. Therefore, the metabolic reaction plays a key role in pharmacological applications of leflunomide, and it is important to understand thoroughly the underlying process of drug action after its intake. Certain attempts have been made in the past to understand this metabolic reaction.[10,11] Many isoxazole ring-containing drugs, including leflunomide, have been reported to undergo reductive ring opening leading to the formation of imine intermediates.[22−24] In the case of leflunomide, the imine intermediates are further converted to *E* and *Z* isomeric forms of the metabolite teriflunomide. The *E* and *Z* forms are interconvertible via a keto tautomer.[17] Conversion of leflunomide to teriflunomide can be both enzymatic (*in vivo*, by the cytochrome P450 enzyme) and

Received: January 20, 2016
Published: March 23, 2016

DOI: 10.1021/acs.jmedchem.6b00088
J. Med. Chem. 2016, 59, 3418−3426

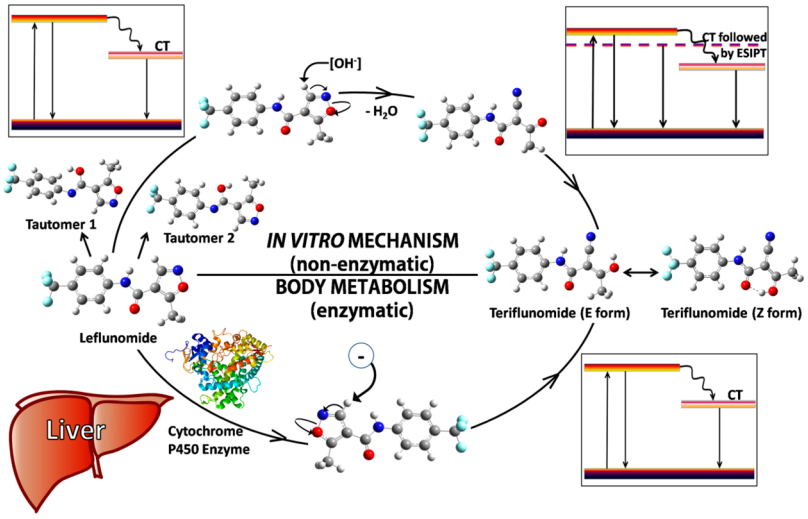

Figure 1. Schematic representation of electronic structures and fluorescence dynamics of the nonenzymatic *in vitro* mechanism of ring opening of leflunomide and comparison with enzymatic *in vivo* metabolism.

nonenzymatic (*in vitro*, in basic media), and it is also influenced by pH and temperature.[10−12] The reaction can be initiated *in vitro* by hydroxyl ions acting as catalysts. Surface-enhanced Raman scattering (SERS) and transition state calculations for this *in vitro* reaction[11] showed the signature of ring opening of leflunomide. However, several aspects have not been understood until now, including the conformational stability of different structural forms produced during the reaction, the excited state behavior of leflunomide and its metabolite, the influence of a change in pH on the reaction, etc. Interestingly, these aspects of leflunomide can be effectively monitored using steady state and time domain fluorescence techniques, which are highly sensitive techniques for understanding changes at the molecular level. Birch et al.[25] demonstrated advancement in a fluorescence technique for *in vivo* metabolic sensing through the photophysics of melanin.

In this work, we have shown that at room temperature the metabolic reaction occurs slowly at neutral pH but is much faster at basic pH. We have focused on monitoring the reaction *in vitro* by studying absorption and fluorescence spectra and performed steady state and time domain fluorescence analyses at neutral as well as basic pH, and the experimental results have been explained with the help of DFT calculations where ground state optimized geometries were obtained and time-dependent DFT (TD-DFT) calculations were performed for absorption spectra at the B3LYP 6-311++G(d,p) level. Solvation in aqueous media was treated using the integral equation formalism of the polarizable continuum model (IEF-PCM). This study reports several new features, e.g., occurrence of excited state twisted intramolecular charge transfer (TICT) in both leflunomide and teriflunomide in aqueous solution, excited state intra/intermolecular proton transfer (ESIPT) during ring opening of leflunomide at basic pH, and *E*−*Z* isomerization of the teriflunomide. The TICT process involves significant electron redistribution, and the ESIPT process involves proton transfer in the excited state causing a large red-shifted emission.[26−31]

RESULTS AND DISCUSSION

Absorption and Steady State Fluorescence Measurements in Aqueous Solution. Absorption spectra of leflunomide and teriflunomide (metabolite) are shown in Figure 2. Leflunomide (10^{-4} M) in aqueous solution has an absorption maximum (λ_{max}) at 258 nm [Figure 2(i)] having a molar extinction coefficient of ∼9500 M^{-1} cm^{-1}, while teriflunomide in aqueous solution has an absorption maximum at 291 nm having a molar absorption coefficient of ∼10500 M^{-1} cm^{-1} [Figure 2(ii)]. It is also noted that in the latter case, the optical density is non-zero unlike that in the former case at the red edge of the absorption spectrum.

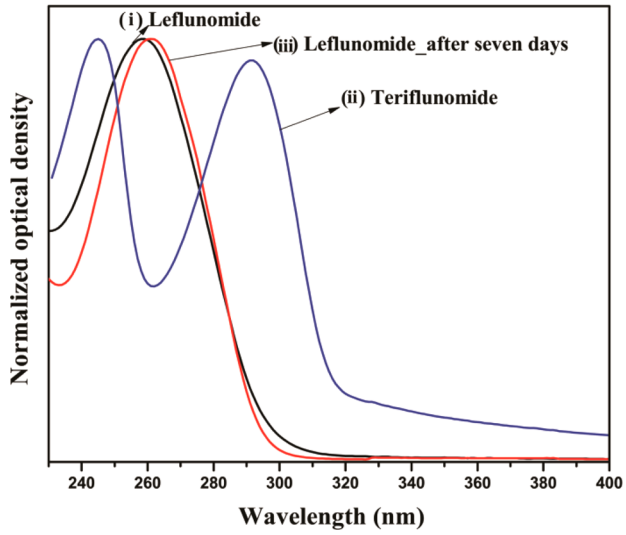

Figure 2. Absorption spectra of (i) leflunomide (10^{-4} M), (ii) teriflunomide (10^{-5} M), and (iii) leflunomide after 7 days in aqueous solution.

The fluorescence emission of leflunomide (10^{-4} M aqueous solution) is large Stokes-shifted emission (∼14600 cm^{-1}) having a λ_{max} at 404 nm (Figure 3a) and an estimated quantum yield of ∼0.36. The fluorescence quantum yield has been calculated with the help of the following equation:

$$\phi = \sum_i \left(\frac{\alpha_i \tau_i}{\alpha_i}\right) \tau_0^{-1}$$

DOI: 10.1021/acs.jmedchem.6b00088
J. Med. Chem. 2016, 59, 3418−3426

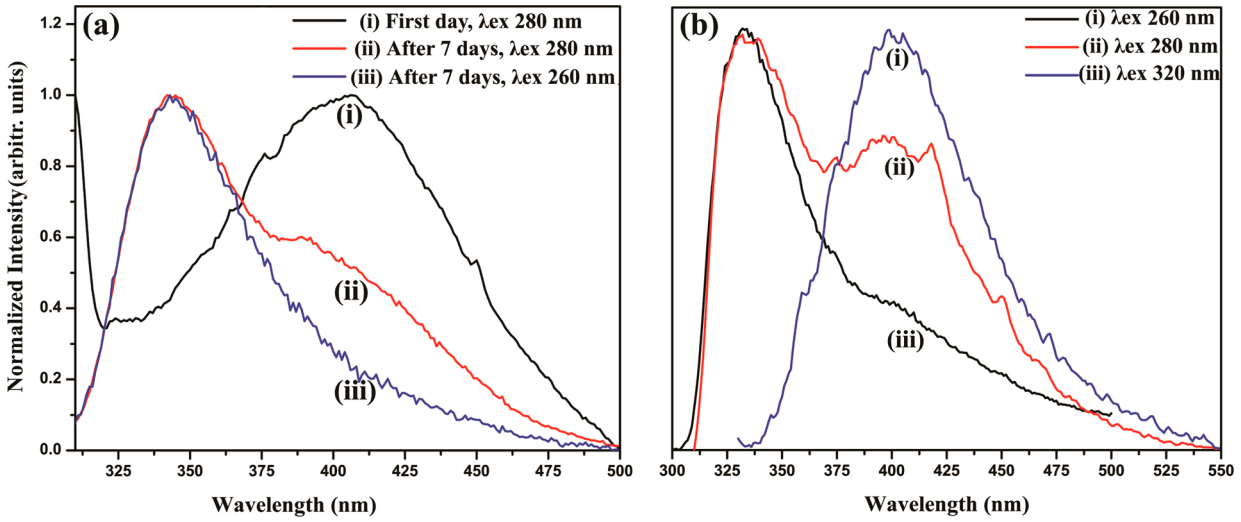

Figure 3. Fluorescence spectra of (a) leflunomide and (b) teriflunomide with different excitation wavelengths.

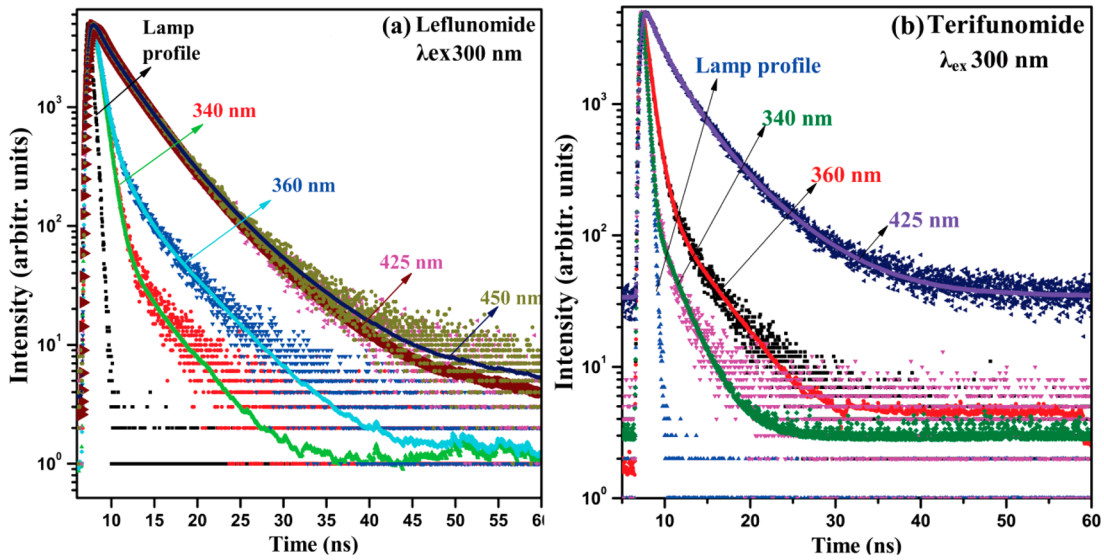

Figure 4. Time-resolved fluorescence decay profiles of (a) leflunomide (10^{-4} M) and (b) teriflunomide (10^{-5} M) monitored at different emission wavelengths with a λ_{ex} of 300 nm.

The values of amplitude α_i and decay times, τ_i's, are taken by analyzed decay profiles (Table S1 of the Supporting Information). Where τ_0 is the calculated radiative decay time, it has been calculated from the well-known Stickler and Berg relation.[32]

$$\tau_0^{-1} = 2.88 \times 10^9 n^2 \left\langle \bar{\upsilon}^{-3} \right\rangle^{-1} \int \frac{\varepsilon(\bar{\upsilon})\, d\bar{\upsilon}}{\bar{\upsilon}}$$

where $\int \frac{\varepsilon(\bar{\upsilon})\, d\bar{\upsilon}}{\bar{\upsilon}}$ represents the area under the first absorption band, $\varepsilon(\bar{\upsilon})$ is the molar extinction coefficient at wavenumber ($\bar{\upsilon}$), and n is the refractive index of the medium.[33−35]

Edge excited red shift (EERS) is observed for this emission profile (Figure S1 of the Supporting Information), and the corresponding shift in excitation profile is also observed. In teriflunomide (10^{-5} M in aqueous solution), on the other hand, wavelength-dependent dual emission at 340 and 400 nm (Figure 3b) is observed without EERS. The Stoke shifts of these bands are 4952 and 9611 cm^{-1}, respectively. The quantum yield of teriflunomide is 0.19, which is less than that of leflunomide by 0.17, which indicates an increase in number of the nonradiative transitions.

It is further observed that after the aqueous solution of leflunomide had been left for a few days at room temperature its absorption band is slightly red-shifted [Figure 2(iii)] and also shows wavelength-dependent dual emission like teriflunomide (Figure 3b). This indicates slow conversion of leflunomide to teriflunomide.

Time Domain Fluorescence Measurements. To understand the fluorescence dynamics of large Stokes-shifted emission and the origin of EERS emission in aqueous medium in leflunomide and dual emission of teriflunomide (at 340 and 400 nm), time domain fluorescence decays were measured at four different emission wavelengths, 340, 360, 425, and 450 nm, using two different available excitation sources, 280 nm (Figure S2 of the Supporting Information) and 300 nm (Figure 4a,b) from a nanosecond pulsed light-emitting diode (LED). We have selected these emission wavelengths to understand the contribution of the different emitting species at different wavelengths. In the case of leflunomide, the decay profiles do

DOI: 10.1021/acs.jmedchem.6b00088
J. Med. Chem. 2016, 59, 3418−3426

Chart 1

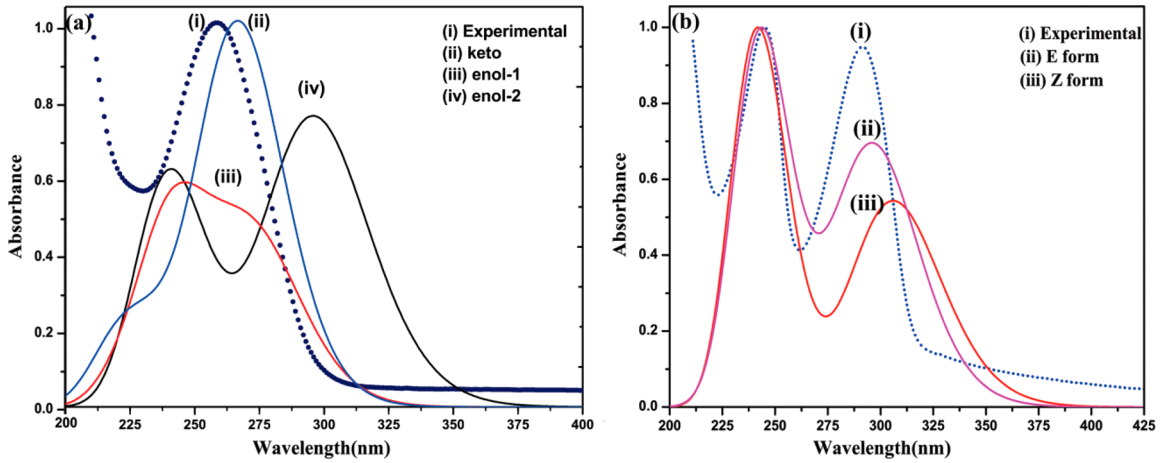

Figure 5. (a) Comparison of experimentally observed absorption spectra of leflunomide with the theoretically calculated spectra of three different tautomers of leflunomide using TD-DFT calculations. (b) Comparison of experimentally observed absorption spectra of teriflunomide with the theoretically calculated absorption spectra of *E* and *Z* forms of teriflunomide using TD-DFT calculations.

not change with a change in the excitation wavelength from 280 to 300 nm, while in the case of teriflunomide, the decay curves are shifted upward and become long upon monitoring the decay at the red edge of the emission spectrum.

A detailed analysis of the decay curves is given in Table S1 of the Supporting Information. Analyses of all the decay profiles for leflunomide, at emission wavelengths of 340 and 360 nm, show the presence of two short-lived components with decay times of ∼0.72 and ∼4.2 ns, but the decay curves at emission wavelengths of 425 and 450 nm were found to have an additional long-lived decay component of ∼6.0 ns as shown in Figure 4a. In the case of teriflunomide, the decay time of emission at 450 nm is longer (∼8.0 ns) than that of leflunomide (Figure 4b). The amplitudes of the shorter decay time components decrease while those of the longer decay time component increase upon going from shorter to longer emission wavelengths in both molecules (Table S1 of the Supporting Information). This indicates that the first and second components belong to the short-lived decay species of leflunomide formed from the ground state due to vertical excitation while the third one belongs to the relaxed excited species. Further, the estimated radiative decay rate of fluorescence of leflunomide ($\sim 1.76 \times 10^8$ s) is found to decrease in teriflunomide ($\sim 8.87 \times 10^7$ s), which causes a decrease in the quantum yield of teriflunomide due to ring opening.

To understand the triple-exponential decay, the fluorescence spectrum of leflunomide was deconvoluted and found to be best fitted with three Gaussian bands, again indicating the presence of three emitting species (Figure S3 of the Supporting Information). The EERS and change in the excitation spectrum support the gradual change in the decay profile at various emission wavelengths with different excitation wavelengths. These results indicate the occurrence of different emitting species of leflunomide. In the case of teriflunomide, with a change in excitation wavelength, a change in the intensities of both the emission peaks is observed. Further, the decay dynamics of leflunomide started to show the same kind of decay behavior as teriflunomide when the aqueous solution of leflunomide was left to stand at room temperature for a few days, supporting transformation of leflunomide to teriflunomide.

Ground and Excited State Electronic Structure Calculations. To understand the nature of absorption spectra and the origin of the large Stokes-shifted emission with multiple decay times, ground and excited state electronic structure calculations were carried out for leflunomide and teriflunomide as discussed below. Leflunomide coexists in one keto form and two enol forms in aqueous solution due to keto−enol tautomerism[17] as shown in Chart 1.

Therefore, geometries of the three conformers of leflunomide were optimized in aqueous solution using the polarizable continuum model (PCM) at the B3LYP/6-311++g(d,p) level of DFT. TD-DFT calculations were conducted to obtain electronic excitation energies and comparison of experimentally (the λ corresponding to the first excitation is at 258 nm) observed absorption spectra of leflunomide with the theoretically calculated absorption spectra of the three different tautomers (the λ corresponding to first excitation is at 267 nm for keto, at 274 nm for enol 1, and at 296 nm for enol 2) of leflunomide mentioned above (Figure 5a). The keto form of leflunomide was found to be most stable, and its enol 1 and enol 2 tautomers were found to be less stable with respect to it by 17.6 and 12.4 kcal/mol, respectively. As the keto tautomer is much more stable than enol tautomers and its theoretical absorption matches nicely experimental absorption spectra, the

DOI: 10.1021/acs.jmedchem.6b00088
J. Med. Chem. 2016, 59, 3418−3426

observed spectral features would be mainly controlled by it. For the optimized planar geometry of the keto form of leflunomide, TD-DFT calculations show the first singlet $\pi \rightarrow \pi^*$ excitation energy to be 267 nm with an oscillator strength of 0.5669. A limited number of steps of optimization of leflunomide in the first excited state in gas phase suggested twisting of the molecule about the C(benzene)−N bond associated with charge transfer (Figure S4a of the Supporting Information). Thus, the first singlet excited state of leflunomide is of the TICT type. TD-DFT calculations revealed the following regarding the nature of TICT in the excited state. (i) In the planar geometry of leflunomide, the HOMO−LUMO excitation is the main contributor to the lowest singlet transition, which transfers a significant amount of electron density from the benzene ring to the attached group containing the isoxazole ring. (ii) In the twisted ground state geometry of leflunomide, several pairs of filled and empty orbitals contribute to the lowest singlet transition, the three main ones being HOMO−1 → LUMO, HOMO−1 → LUMO+1, and HOMO−2 → LUMO+1 (Figure 6a). The first of these two

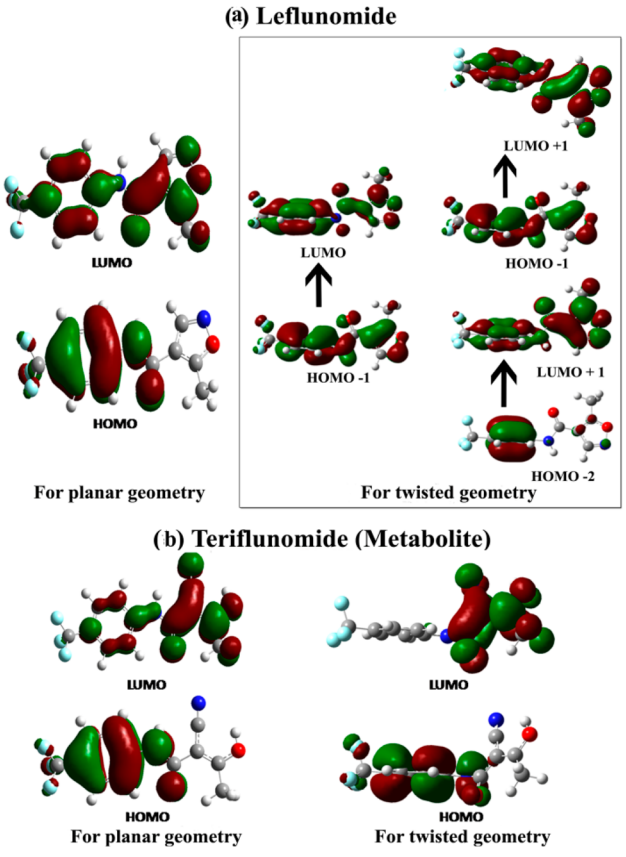

Figure 6. Orbitals involved in the lowest singlet transitions having TICT character in (a) leflunomide and (b) teriflunomide.

excitations maintains the charge transfer, while the third enhances the same. Thus, the lowest singlet excited state of the molecule is further established to be of the TICT type. It shows that the large Stokes-shifted emission around 404 nm arises from the TICT-relaxed excited state of leflunomide.

Similar to leflunomide, twisting about the C(benzene)−N bond also takes place in the lower singlet excited state of teriflunomide as revealed by TD-DFT calculations (Figure 6b). In both planar and twisted geometries, the HOMO−LUMO orbital pairs are involved in the first singlet transition, and in both the cases, the transitions are of the TICT type, transferring electron density from the benzene ring to the corresponding attached group (Figure 6b). Teriflunomide exists in two interconvertible *E* and *Z* enol forms as shown in Chart 2.

Chart 2

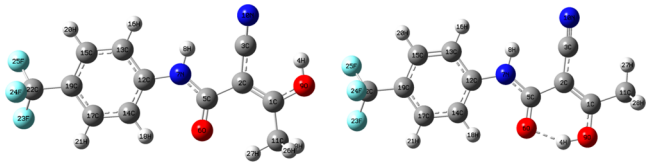

The *Z* form is more stable by ∼10 kcal/mol than the *E* form of teriflunomide because of the presence of a strong intramolecular O−H···O (1.91 Å) hydrogen bond. A comparison of the theoretically calculated absorption spectra of both the *E* and *Z* forms using the corresponding ground state optimized geometries in aqueous solution shows a red-shifted absorption by the *Z* form (306 nm) compared to that of the *E* form (296 nm), and their combined absorption spectrum resembles that of teriflunomide in aqueous solution (Figure 5b). Upon comparison of these results with experimental absorption spectra, the non-zero optical density at longer wavelengths suggests the coexistence of both *E* and *Z* enolic forms of teriflunomide in aqueous solution. The large Stokes-shifted emission of teriflunomide also can be interpreted as arising from the TICT-relaxed excited state. The presence of the two (*E* and *Z*) forms can also be confirmed by changing the excitation wavelengths. When a wavelength of 260 nm is used for excitation, an intense emission at 340 nm with a hump at 400 nm is observed (Figure 3b), while when a wavelength of 320 nm is used for excitation, the intensity of the 400 nm emission peak increases. This wavelength-dependent dual emission of teriflunomide indicates that the 340 nm emission arises due to the *E* form while the 400 nm emission arises due to the *Z* form of teriflunomide.

Ring Opening of Leflunomide at Basic pH. Upon addition of the buffer solution at pH 10 in the fresh aqueous solution of leflunomide (10^{-4} M), the 258 nm absorption band started to split into two bands (at 246 and 291 nm) along with an increase in intensity near the red edge of the absorption band during the metabolic reaction (Figure 7a), and it finally resembles the absorption spectrum of teriflunomide. During this reaction, the intensity of the 258 nm band decreases while those of the 246 and 291 nm bands increase (inset of Figure 7a). After 120 min, there was no observed change in the optical density at 258 and 291 nm, which shows the saturation of the reaction.

The single large Stokes-shifted fluorescence band of leflunomide also started to convert into two bands appearing at 340 and 425 nm upon addition of the buffer solution at pH 10 as shown in Figure 7b. The variation of the ratio of fluorescence intensities at 340 and 425 nm with time (I_{340}/I_{425}) is shown in the inset of Figure 7b. This dual fluorescence of leflunomide at pH 10 resembles the fluorescence spectrum of teriflunomide, although the emission at 400 nm is found to be ∼25 nm red-shifted with respect to that of teriflunomide in aqueous solution. This observation can be explained as follows.

DOI: 10.1021/acs.jmedchem.6b00088
J. Med. Chem. 2016, 59, 3418−3426

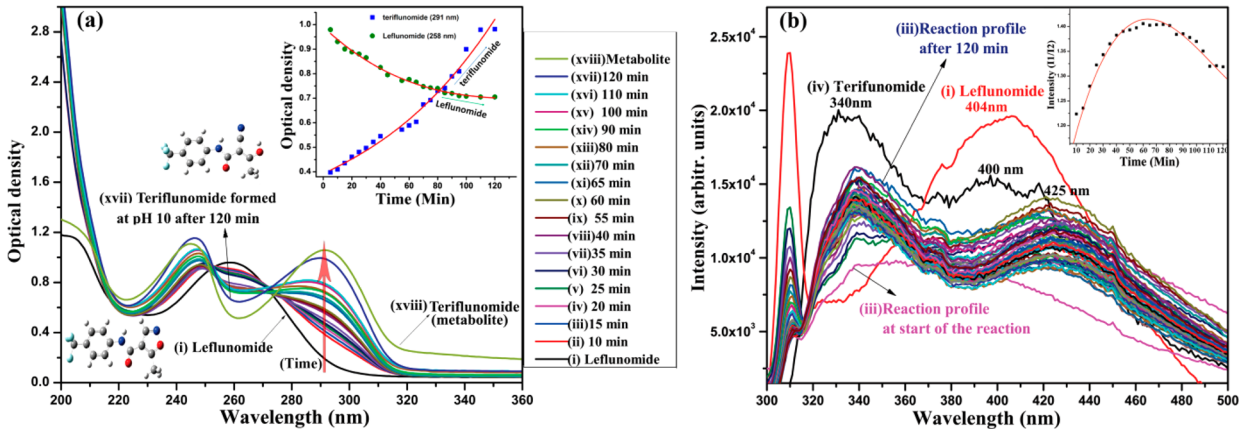

Figure 7. Time series (a) absorption and (b) emission spectra of a 10^{-4} M aqueous solution of leflunomide at pH 10 with overlapped absorption and emission spectra of leflunomide and teriflunomide.

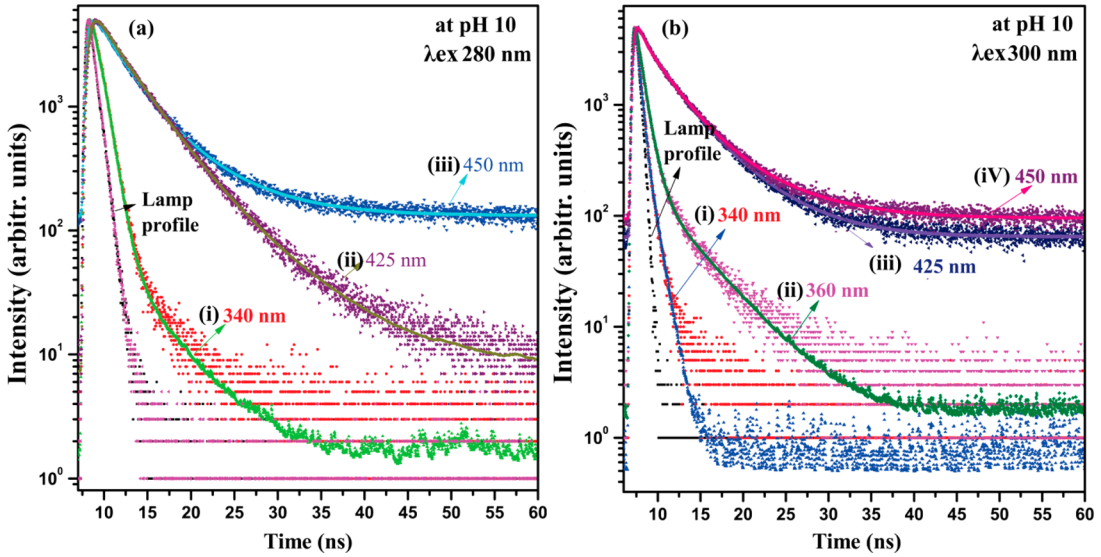

Figure 8. Time-resolved fluorescence decay profiles of leflunomide (10^{-4} M) monitored at different emission wavelengths at pH 10: (a) λ_{ex} = 280 nm, and (b) λ_{ex} = 300 nm.

Because of the catalytic effect of OH^- ions, a negative charge develops at the C3 site (Chart 1), which results in intramolecular proton transfer in leflunomide. It causes the isoxazole ring of leflunomide to open and convert to teriflunomide. In this reaction, leflunomide is first converted to the *E* form of teriflunomide by TICT, and subsequently, the *E* form is converted to the *Z* form by ESIPT. Thus, TICT and ESIPT are coupled and produce the *Z* form of teriflunomide, which results in the large Stokes-shifted emission at 425 nm.

It is well-known from the Beer–Lambert law that the optical density is directly proportional to the concentration of the solute. Therefore, to understand the kinetics of this metabolic reaction, we have focused on the change in optical density with time (inset of Figure 7a). This indicates an increase in the amount of teriflunomide and a simultaneous decrease in the amount of leflunomide in aqueous solution during the reaction. At the start of the reaction, the concentration of leflunomide was 1×10^{-4} M. We estimated the approximate concentration of teriflunomide when the optical density after ~120 min was nearly constant and determined its value to be $\sim 0.95 \times 10^{-4}$ M. This indicated that nearly complete transformation of leflunomide to teriflunomide had taken place.

Fitting of the curves shows that the optical density of the 258 nm band of leflunomide decreases exponentially, while those of the 246 and 291 nm bands of teriflunomide increase exponentially with time. Upon comparing these results with the scheme of this reaction presented in Figure 1, we observed that leflunomide is first converted into the *E* form of teriflunomide with a fast rate due to the catalytic action of OH^- up to 80 min, and after that, intramolecular proton transfer leads to slow conversion of the *E* form to the *Z* form of teriflunomide. In support of the results presented above, the intensity ratio of the two fluorescence bands (I_{340}/I_{425}) is plotted as a function of time in the inset of Figure 7b. As explained earlier, the emission at 340 nm is due to the *E* form while that at 425 nm is due to the *Z* form. The I_{340}/I_{425} ratio initially increases for ~80 min and subsequently decreases when ESIPT takes over, and the *Z* form of teriflunomide is formed.

Time-resolved fluorescence measurements on an aqueous leflunomide solution were taken after pH 10 buffer had been added at different time intervals at four different emission wavelengths, viz., 340, 360, 425, and 450 nm, with excitation wavelengths of 280 and 300 nm. The decay curves recorded

DOI: 10.1021/acs.jmedchem.6b00088
J. Med. Chem. 2016, 59, 3418–3426

120 min after the addition of pH 10 buffer are shown in panels a and b of Figure 8. The decay curve resembles that of teriflunomide with a further increase in decay time at the red edge of longer emission. Faster decay of 340 and 360 nm emissions indicates that the emissions arise from the initially excited *E* form of teriflunomide. The relaxed emission at 425 nm by 280 nm excitation shows the emission from the TICT state during the conversion of the *E* form to the *Z* form, and a further increase in the decay time of 450 nm emission occurs due to TICT followed by ESIPT in the *Z* form of teriflunomide. Upon using 300 nm excitation, only decay corresponding to the ESIPT state in the *Z* form is observed. The decay profiles have the same appearance as the decay curves of teriflunomide at emission wavelengths of 340 and 425 nm (Figure 4b). Further, the decay profile was also recorded at 400 nm using a 375 nm picosecond pulsed laser excitation, which does not change with time but varies at different emission wavelengths (400 and 440 nm) in a similar way as for the 300 nm excitation from the relaxed species (Figure S5 of the Supporting Information). Thus, the fluorescence lifetime is independent of the process of ring opening of leflunomide.

Reaction at pH 11 and 12. To investigate the pH dependence of the transformation of leflunomide to teriflunomide, the reaction was further monitored by studying absorption and fluorescence spectra at pH 11 and 12 (Figure S6 of the Supporting Information). We observed changes in the spectra with respect to time similar to those at pH 10, but the time of completion of the reaction was much less at pH 11 and 12. Absorption spectra showed that the formation of teriflunomide from leflunomide reached completion after only 35 and 15 min at pH 11 and 12, respectively. Moreover, at these pH values, the intensity of the 340 nm emission peak increases sharply while the 425 nm peak appears slowly and gradually becomes intense with the passage of time. Obviously, a stronger catalytic action at pH 11 and 12 results in a faster conversion of leflunomide to the *E* form of teriflunomide.

CONCLUSION

The results of this study are schematically summarized in Figure 1. The bottom half of the scheme depicts how leflunomide after intake is converted to *E* and *Z* forms of its active metabolite teriflunomide in the presence of the cytochrome P450 enzyme *in vivo*. The same reaction has been studied *in vitro* via base catalysis as shown in the top half of the scheme with the help of electronic structure calculations and steady state/time-resolved fluorescence spectroscopy. Leflunomide may exist in one keto and two enol forms in aqueous solution that are simultaneously converted through isoxazole ring opening to *E* and *Z* forms of teriflunomide. In this process, the catalytic OH^- ions cause cleavage of the N−O bond of the isoxazole ring and formation of the *E* and *Z* forms of teriflunomide. The geometrical changes during the process have been monitored through the changes in fluorescence dynamics, and these and different photophysical processes are indicated in the energy level diagrams in Figure 1.

It is found that conversion of leflunomide to teriflunomide occurs in aqueous solution even without the addition of the basic pH buffer. However, the reaction rate is much faster at basic pH where the *E* and *Z* forms of teriflunomide are more stabilized. Charge transfer (TICT) followed by proton transfer (ESIPT) was observed in the reaction solution at basic pH. With an increase in the basicity of the medium, the reaction rate further increases and the *E* form of teriflunomide is found to be more stable at the start of the reaction. As the *E* form of teriflunomide is more potent, we conclude that the action of leflunomide can be enhanced by increasing the basicity of the medium. This study reveals several interesting facts about the excited state reaction dynamics that was unexplored until now. It is expected to open the scope for further research concerned with the pharmacological applications of leflunomide and also of other important drug molecules with the help of absorption and fluorescence techniques.

EXPERIMENTAL DETAILS

Leflunomide was purchased from BIOTREND, Germany, and teriflunomide was purchased from Sigma-Aldrich, India, and used without further purification. The absorption spectra were recorded using a PerkinElmer UV−vis Lambda 25 spectrophotometer. Emission and excitation spectra were recorded using an Edinburg FLS 900 fluorescence spectrophotometer with a xenon source for excitation from the Photonics Division of Edinburgh Instruments. All the fluorescence measurements were taken with a spectral slit width of 4 nm, in both the excitation monochromator and the emission monochromator channels. Fluorescence decays were measured using an Edinburgh FLS 900 fluorescence spectrophotometer and a Horiba deltaflex fluorescence lifetime system using the time-correlated single-photon counting (TCSPC) technique with the TBX picosecond detection module. The excitation sources were light-emitting diodes (Delta LED) having sharp emission with a low full width at half-maximum of two wavelengths, viz. 280 and 300 nm, and a 375 nm picosecond laser.

THEORETICAL DETAILS

Geometry optimization and vibrational frequency calculations on keto, enol 1, and enol 2 forms of leflunomide and *E* and *Z* forms of teriflunomide were performed in the gas phase using Becke's[36] nonlocal three-parameter exchange correlation functional along with the Lee−Yang−Parr correlation functional (B3LYP)[37] with the 6-311++G(d,p) basis set. All the theoretical calculations were performed using Gaussian 03.[38] For visualization of optimized structures and vibrational modes, GaussView version 4.2 was used.[39] For each optimized structure, a frequency analysis at the same level of theory was used to verify that it corresponds to a minimum in the potential energy surface. As there were no imaginary frequencies found. Excited state properties, e.g., excitation energies and oscillator strengths, were calculated with the time-dependent density functional (TD-DFT) formalism.[40−42] To incorporate the bulk solvent effect of water on the properties of leflunomide and teriflunomide, the polarizable continuum model (PCM)[43] was employed. All the ground state geometries were optimized in aqueous media. In PCM,[43] the solute is placed in a cavity formed in the continuous solvent medium and both the solute and solvent polarize each other, producing a charge distribution at the cavity surface that perturbs the solute.

ASSOCIATED CONTENT

Supporting Information

The Supporting Information is available free of charge on the ACS Publications website at DOI: 10.1021/acs.jmedchem.6b00088.

Analyzed decay data of leflunomide (10^{-4} M), leflunomide (10^{-4} M) at pH 10, and teriflunomide (10^{-5} M) in aqueous solution (Table S1); normalized emission spectra of leflunomide (10^{-4} M) in aqueous solution excited by three different wavelengths (λ_{ex} = 280, 300, and 320 nm) (Figure S1); time-resolved

DOI: 10.1021/acs.jmedchem.6b00088
J. Med. Chem. 2016, 59, 3418−3426

fluorescence decay profiles of leflunomide (10^{-4} M) monitored at different emission wavelengths with a λ_{ex} of 280 nm (Figure S2); deconvoluted emission band of leflunomide (10^{-4} M) (Figure S3); optimized structures of planar and twisted geometries of leflunomide and teriflunomide (Figure S4); decay curves of a leflunomide (10^{-4} M) aqueous solution at pH 10, emission at two wavelengths (viz. 400 and 440 nm), time-dependent decay profile with emission at 400 nm, and distribution of residuals and χ^2 for best fit decay functions (triple exponential) below the decay curves (Figure S5); and absorption and fluorescence spectra of time-dependent metabolic reaction of leflunomide at pH 11 and 12 (Figure S6) (PDF)

AUTHOR INFORMATION

Corresponding Authors

*Telephone: +919454161037. E-mail: hmishra@bhu.ac.in.
*Telephone: +91542-6701569. E-mail: ranjanksingh65@rediffmail.com.

Author Contributions

P.S. and D.G. have contributed equally to this work.

Notes

The authors declare no competing financial interest.

ACKNOWLEDGMENTS

The authors thank Dr. M. S. Mehata (DTU, Delhi, India) for some of the time domain fluorescence measurements. D.G. is grateful to CSIR, India, for providing a senior research fellowship. R.K.S. is grateful to the AvH Foundation, Germany, and DST, India (DST-FIST Scheme). H.M. is thankful to UGC, India, for providing project funds. P.C.M. thanks the National Academy of Sciences, India, for a senior scientist fellowship.

ABBREVIATIONS USED

FDA, Food and Drug Administration; NMR, nuclear magnetic resonance; DHODH, dihydroorotate dehydrogenase; DFT, density functional theory; XRD, X-ray diffraction; SERS, surface-enhanced Raman scattering; TD-DFT, time-dependent density functional theory; IEF-PCM, integral equation formalism of the polarizable continuum model; TICT, twisted intramolecular charge transfer; ESIPT, excited state intra/intermolecular proton transfer; EERS, edge excitation red shift; HOMO, highest occupied molecular orbital; LUMO, lowest unoccupied molecular orbital

REFERENCES

(1) Davis, J. P.; Cain, G. A.; Pitts, W. J.; Magolda, R. L.; Copeland, R. A. The immunosuppressive metabolite of leflunomide is a potent inhibitor of human dihydroorotate dehydrogenase. *Biochemistry* **1996**, *35*, 1270−1273.

(2) Rozman, B. Clinical experience with leflunomide in rheumatoid arthritis. Leflunomide Investigators' Group. *J. Rheumatol. Suppl.* **1998**, *53*, 27−32.

(3) Rozman, B. Clinical pharmacokinetics of leflunomide. *Clin. Pharmacokinet.* **2002**, *41*, 421−430.

(4) Dimitrijevic, M.; Bartlett, R. R. Leflunomide, a novel immunomodulating drug, inhibits homotypic adhesion of peripheral blood and synovial fluid mononuclear cells in rheumatoid arthritis. *Inflammation Res.* **1996**, *45*, 550−556.

(5) Breedveld, F. C.; Dayer, J. M. Leflunomide: mode of action in the treatment of rheumatoid arthritis. *Ann. Rheum. Dis.* **2000**, *59*, 841−849.

(6) Baumann, P.; Mandl-Weber, S.; Völkl, A.; Adam, C.; Bumeder, I.; Oduncu, F.; Schmidmaier, R. Dihydroorotate dehydrogenase inhibitor A771726 (leflunomide) induces apoptosis and diminishes proliferation of multiple myeloma cells. *Mol. Cancer Ther.* **2009**, *8*, 366−375.

(7) Fuentealba, R. A.; Marasa, J.; Diamond, M. I.; Piwnica-Worms, D.; Weihl, C. C. An aggregation sensing reporter identifies leflunomide and teriflunomide as polyglutamine aggregate inhibitors. *Hum. Mol. Genet.* **2012**, *21*, 664−680.

(8) Cutolo, M.; Sulli, A.; Ghiorzo, P.; Pizzorni, C.; Craviotto, C.; Villaggio, B. Anti-inflammatory effects of leflunomide on cultured synovial macrophages from patients with rheumatoid arthritis. *Ann. Rheum. Dis.* **2003**, *62*, 297−302.

(9) Bernhoff, E.; Tylden, G. D.; Kjerpeseth, L. J.; Gutteberg, T. J.; Hirsch, H. H.; Rinaldo, C. H. Leflunomide inhibition of BK virus replication in renal tubular epithelial cells. *J. Virol.* **2010**, *84*, 2150−2156.

(10) Kalgutkar, A. S.; Nguyen, H. T.; Vaz, A. D. N.; Doan, A.; Dalvie, D. K.; Mcleod, D. G.; Murray, J. C. In-vitro metabolism studies on the isoxazole ring scission in the anti-inflammatory agent leflunomide to its active-cyanoenol metabolite A771726: Mechanistic similarities with the cytochrome P450-catalyzed dehydration of aldoximes. *Drug Metab. Dispos.* **2003**, *31*, 1240−1250.

(11) Sharma, P.; Gangopadhyay, D.; Singh, P.; Mishra, P. C.; Deckert, V.; Popp, J.; Singh, R. K. In vitro monitoring of ring opening of leflunomide: A surface enhanced Raman scattering and DFT based approach. *Chem. Phys. Lett.* **2014**, *613*, 127−132.

(12) Yu, J.; Folmer, J. J.; Hoesch, V.; Doherty, J.; Campbell, J. B.; Burdette, D. Elucidation of a novel bioactivation pathway of a 3,4-unsubstituted isoxazole in human liver microsomes: Formation of a glutathione adduct of a cyanoacrolein derivative after isoxazole ring opening. *Drug Metab. Dispos.* **2011**, *39*, 302−311.

(13) O'Connor, P. W.; Li, D.; Freedman, M. S.; Bar-or, A.; Rice, G. P. A.; Confavreux, C.; Paty, D. W.; Stewart, J. A.; Scheyer, R. A Phase II study of the safety and efficacy of teriflunomide in multiple sclerosis with relapses. *Neurology* **2006**, *66*, 894−900.

(14) McLean, J. E.; Neidhardt, E. A.; Grossman, T. H.; Hedstrom, L. Multiple inhibitor analysis of the brequinar and leflunomide binding sites on human dihydroorotate dehydrogenase. *Biochemistry* **2001**, *40*, 2194−2200.

(15) Davies, M.; Heikkilä, T.; McConkey, G. A.; Fishwick, C. W.; Parsons, M. R.; Johnson, A. P. Structure-based design, synthesis, and characterization of inhibitors of human and *Plasmodium falciparum* dihydroorotate dehydrogenases. *J. Med. Chem.* **2009**, *52*, 2683−2693.

(16) Liu, S.; Neidhardt, E. A.; Grossman, T. H.; Ocain, T.; Clardy, J. Structures of human dihydroorotate dehydrogenase in complex with antiproliferative agents. *Structure* **2000**, *8*, 25−33.

(17) Kujawski, J.; Bernard, M. K.; Jodłowska, E.; Czaja, K.; Drabińska, B. On the interactions of leflunomide and teriflunomide within receptor cavity-NMR studies and energy calculations. *J. Mol. Model.* **2015**, *21*, 105.

(18) Raissi, H.; Mollania, F. Immunosuppressive agent leflunomide: a SWNTs-immobilized dihydroortate dehydrogenase inhibitory effect and computational study of its adsorption properties on zigzag single walled (6,0) carbon and boron nitride nanotubes as controlled drug delivery devices. *Eur. J. Pharm. Sci.* **2014**, *56*, 37−54.

(19) Panek, J. J.; Jezierska, A.; Mierzwicki, K.; Latajka, Z.; Koll, A. Molecular modeling study of leflunomide and its active metabolite analogues. *J. Chem. Inf. Model.* **2005**, *45*, 39−48.

(20) Vega, D.; Petragalli, A.; Fernández, D.; Ellena, J. A. Polymorphism on leflunomide: stability and crystal structures. *J. Pharm. Sci.* **2006**, *95*, 1075−1083.

(21) Sharma, P.; Gangopadhyay, D.; Umrao, S.; Kumar, S.; Ghosh, A. K.; Mishra, P. C.; Singh, R. K. A novel Raman spectroscopic approach to identify polymorphism in leflunomide: a combined experimental and theoretical study. *J. Raman Spectrosc.* **2015**, n/a.

DOI: 10.1021/acs.jmedchem.6b00088
J. Med. Chem. 2016, 59, 3418−3426

(22) Stiff, D. D.; Zemaitis, M. A. Metabolism of the anticonvulsant agent zonisamide in the rat. *Drug Metab. Dispos.* **1990**, *18*, 888−894.
(23) Mannens, G.; Huang, M. L.; Meuldermans, W.; Hendrickx, J.; Woestenborghs, R.; Heykants, J. Absorption, metabolism, and excretion of risperidone in humans. *Drug Metab. Dispos.* **1993**, *21*, 1134−1141.
(24) Boucher, J. L.; Delaforge, M.; Mansuy, D. Dehydration of alkyl- and arylaldoximes as a new cytochrome P450-catalyzed reaction: mechanism and stereochemical characteristics. *Biochemistry* **1994**, *33*, 7811−7818.
(25) Birch, D. J. S.; Ganesan, A.; Karolin, J. Metabolic sensing using fluorescence. *Synth. Met.* **2005**, *155*, 410−413.
(26) Shigemitsu, Y.; Mutai, T.; Houjou, H.; Araki, K. Excited-state intramolecular proton transfer (ESIPT) emission of hydroxyphenylimidazopyridine: Computational study on enhanced and polymorph-dependent luminescence in the solid state. *J. Phys. Chem. A* **2012**, *116*, 12041−12048.
(27) Majumdar, P.; Zhao, J. 2-(2-hydroxyphenyl)-benzothiazole (HBT)-rhodamine dyad: acid-switchable absorption and fluorescence of excited-state intramolecular proton transfer (ESIPT). *J. Phys. Chem. B* **2015**, *119*, 2384−2394.
(28) Nikolaev, A. E.; Myszkiewicz, G.; Berden, G.; Meerts, W. L.; Pfanstiel, J. F.; Pratt, D. W. Twisted intramolecular charge transfer states: Rotationally resolved fluorescence excitation spectra of 4, 4′-dimethylaminobenzonitrile in a molecular beam. *J. Chem. Phys.* **2005**, *122*, 084309−084312.
(29) Manz, J.; Proppe, B.; Schmidt, B. Time-resolved dual fluorescence of 1-phenylpyrrole in acetonitrile: molecular dynamics simulations of solvent response to twisted intramolecular charge transfer. *Phys. Chem. Chem. Phys.* **2002**, *4*, 1876−1881.
(30) Mishra, H.; Pant, D.; Pant, T. C.; Tripathi, H. B. Edge excitation red shift and energy migration in quinine bisulphate dication. *J. Photochem. Photobiol., A* **2006**, *177*, 197−204.
(31) Misra, V.; Mishra, H. Photoinduced proton transfer coupled with energy transfer:Mechanism of sensitized luminescence of terbium ion by salicylic acid doped in polymer. *J. Chem. Phys.* **2008**, *128*, 244701.
(32) Strickler, S. J.; Berg, R. A. Relationship between absorption intensity and fluorescence lifetime of molecules. *J. Chem. Phys.* **1962**, *37*, 814−822.
(33) Birks, J. B. *Organic Molecular Photophysics*; John Wiley & Sons: New York, 1973.
(34) Lakowicz, J. R. *Principles of Fluorescence Spectroscopy*, 3rd ed.; Springer: New York, 2006.
(35) Mishra, H.; Pant, S.; Tripathi, H. B. Temperature-dependent time-resolved fluorescence study of cinchonine alkaloid dication. *J. Fluoresc.* **2008**, *18*, 17−28.
(36) Becke, A. D. Density functional thermochemistry. III. The role of exact exchange. *J. Chem. Phys.* **1993**, *98*, 5648−5652.
(37) Lee, C.; Yang, W.; Parr, R. G. Development of the Colle-Salvetti correlation-energy formula into a functional of the electron density. *Phys. Rev. B: Condens. Matter Mater. Phys.* **1988**, *37*, 785−789.
(38) Frisch, M. J.; Trucks, G. W.; Schlegel, H. B.; Scuseria, G. E.; Robb, M. A.; Cheeseman, J. R.; Zakrzewski, V. G.; Montgomery, J. A., Jr.; Stratmann, R. E.; Burant, J. C.; Dapprich, S. J.; Millam, M.; Daniels, A. D.; Kudin, K. N.; Strain, M. C.; Farkas, O.; Tomasi, J.; Barone, V.; Cossi, M.; Cammi, R.; Mennucci, B.; Pomelli, C.; Adamo, C.; Clifford, S.; Ochterski, J.; Petersson, G. A.; Ayala, P. Y.; Cui, Q.; Morokuma, K.; Malick, D. K.; Rabuck, A. D.; Raghavachari, K.; Foresman, J. B.; Cioslowski, J.; Ortiz, J. V.; Baboul, A. G.; Stefanov, B. B.; Liu, G.; Liashenko, A.; Piskorz, P.; Komaromi, I.; Gomperts, R.; Martin, R. L.; Fox, D. J.; Keith, T.; Al-Laham, M. A.; Peng, C. Y.; Nanayakkara, A.; Challacombe, M.; Gill, P. M. W.; Johnson, B.; Chen, W.; Wong, M. W.; Andres, J. L.; Gonzalez, C.; Head-Gordon, M.; Replogle, E. S.; Pople, J. A. *Gaussian 03*; Gaussian, Inc.: Pittsburgh, PA, 2003.
(39) Dennington, R., II; Keith, T.; Millam, J.; Eppinnett, K.; Hovell, W. L.; Gilliland, R. *GaussView*, version 4.1; Semichem, Inc.: Shawnee Mission, KS, 2003.
(40) Ricciardi, G.; Rosa, A.; Van Gisbergen, S. J.; Baerends, E. J. A density functional study of the optical spectra and nonlinear optical properties of heteroleptic tetrapyrrole sandwich complexes: The porphyrinato−porphyrazinato−zirconium(IV) complex as a case study. *J. Phys. Chem. A* **2000**, *104*, 635−643.
(41) Van Gisbergen, S. J. A.; Groeneveld, J. A.; Rosa, A.; Snijders, J. G.; Baerends, E. J. Excitation energies for transition metal compounds from time-dependent density functional theory. Applications to MnO_4-, $Ni(CO)_4$, and $Mn2(CO)_{10}$. *J. Phys. Chem. A* **1999**, *103*, 6835−6844.
(42) Rosa, A.; Baerends, E. J.; Van Gisbergen, S. J. A.; van Lenthe, E.; Groeneveld, J. A.; Snijders, J. G. Electronic spectra of $M(CO)_6$ (M = Cr, Mo, W) revisited by a relativistic TDDFT approach. *J. Am. Chem. Soc.* **1999**, *121*, 10356−10365.
(43) Tomasi, J.; Mennucci, B.; Cammi, R. Quantum mechanical continuum solvation models. *Chem. Rev.* **2005**, *105*, 2999−3094.

DOI: 10.1021/acs.jmedchem.6b00088
J. Med. Chem. 2016, 59, 3418−3426